Results in Engineering 18 (2023) 101123

Contents lists available at ScienceDirect

Results in Engineering

journal homepage: www.sciencedirect.com/journal/results-in-engineering

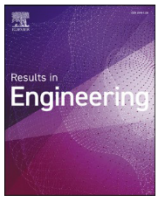

Effects of teff straw ash on the mechanical and microstructural properties of ambient cured fly ash-based geopolymer mortar for onsite applications

Tajebe Bezabih [a,*], Christopher Kanali [b], Joseph Thuo [c]

[a] Department of Civil Engineering, Pan African University Institute for Basic Sciences, Technology and Innovation (PAUSTI), Nairobi, Kenya
[b] Department of Agricultural and Biosystems Engineering, Jomo Kenyatta University of Agriculture & Technology (JKUAT), Nairobi, Kenya
[c] Department of Civil Engineering, Dedan Kimathi University of Technology (DeKUT), Nyeri, Kenya

ARTICLE INFO

Keywords:
Teff straw ash
Compressive strength
Fly ash
Cement
Geopolymer
Microstructure
Ambient curing

ABSTRACT

Although geopolymer cement (GPC) is a substitute for Portland cement, its application is restricted due to the need for high-temperature curing (40–90 °C), which makes it challenging to utilise for onsite applications. To address this issue, the current study examined the potential of substituting fly ash (FA) with teff straw ash (TSA) in geopolymer mortars cured at ambient temperature. The findings revealed that substituting FA with TSA can eliminate the need for high-temperature curing, and the compressive strengths of FA-TSA-based geopolymer mortar mixtures cured for 28 days ranged from 45 to 53 MPa. Further, increasing the TSA content enhanced the mortar's flexural and direct tensile strengths. A teff straw ash level of 10% increased compressive, flexural, and direct tensile strengths by 40%, 59%, and 30% at 28 days, respectively. Furthermore, the mineralogical phases of the mortar after 28 days confirmed the presence of gismondine coexisting with other phases, and microstructural analysis indicates that the inclusion of TSA resulted in a denser structure. These findings suggest that TSA could be a potential substitute for FA in GPC applications to lower energy usage and environmental impact.

1. Introduction

Concrete, following water, stands as the second most extensively employed material across the globe [1–4]. Concrete production typically relies on two common binding materials: Ordinary Portland cement (OPC) and Portland pozzolan cement (PPC). As long as concrete remains a preferred option in the construction industry, the demand for Portland cement as a binder continues to increase accordingly. Reports indicate that cement production has increased from about 1.2 billion tonnes in 1990 and is expected to reach 5.8 billion tonnes in 2050 [5].

The issue of climate change and the need for environmental conservation has emerged as a significant concern. Human activities, including the emission of harmful pollutants such as carbon dioxide (CO_2) into the air, play a critical role in triggering the concerning phenomenon of global warming. CO_2 accounts for around 65% of the global temperature rise from greenhouse gases [6]. Due to the calcination of limestone and the significant energy requirements, the manufacture of Portland cement generates 7–10% of the total CO_2 emissions [7–9]. According to the reported estimates, a tonne of CO_2 is emitted, and two tonnes of natural resources are utilised to manufacture one metric tonne of cement [10]. Furthermore, for environmental sustainability, improper waste disposal and industrial by-product materials must be prevented [11]. Therefore, efforts are ongoing to ensure the reduction of cement usage in the construction industry. This involves exploring alternatives such as supplementary cementing materials and substitutes for Portland cement binders. In this regard, geopolymer cement has been seen as an alternative binder for construction and infrastructure purposes with a significantly lower environmental impact when compared to Portland cement [12].

Geopolymer cement, a novel material used to substitute Portland cement, can be manufactured by activating various aluminosilicate source materials that differ in reactivity, availability, cost, application, and quantity around the world with an alkaline activator solution at an optimal curing temperature [13]. Geopolymer cement, as a cementitious material, is known to be more environmentally friendly than Portland cement for several reasons. Geopolymer cement production typically involves lower carbon emissions as it requires lower temperatures than Portland cement production, reducing greenhouse gas emissions. Moreover, geopolymer has the potential to utilise industrial by-products or waste materials, reducing the need for resource extraction and waste disposal. Geopolymer-based materials also offer excellent durability, better thermal insulation properties, and potential for land reclamation,

* Corresponding author.
E-mail address: tajebe12@gmail.com (T. Bezabih).

https://doi.org/10.1016/j.rineng.2023.101123
Received 22 March 2023; Received in revised form 23 April 2023; Accepted 23 April 2023
Available online 25 April 2023
2590-1230/© 2023 The Authors. Published by Elsevier B.V. This is an open access article under the CC BY-NC-ND license (http://creativecommons.org/licenses/by-nc-nd/4.0/).

making them a sustainable choice for construction [14].

Studies have shown that geopolymer cement can significantly reduce CO_2 emissions by up to 80% compared to Portland cement and uses 59% less energy during production [15]. Another crucial feature of geopolymer cement is its ability to cure without water [16]. Additionally, geopolymer cement utilises waste materials that are a massive threat to environmental stability and human health, which include oil shale ash, fly ash (FA), ground granulated blast-furnace slag (GGBFS), rice husk ash (RHA), silica fume, and metakaolin (MK) [17]. In addition to waste materials, natural resources, including kaolin [18], zeolite [19], laterite soil [20], and others, are also used in the production of geopolymers.

Fly ash is a residue produced when coal is combusted for energy production, and it has been identified as a pollutant to the environment. Fly ash has an annual production estimate of 2.8 billion metric tonnes per year [21]. Fly ash has some major and minor elements. The major components are SiO_2, Al_2O_3, Fe_2O_3, and CaO and are present in crystalline and amorphous oxides and other varied minerals [22]. On the other hand, minor elements may be toxic, some of which are Pb, As, Hg, and Cr. As a result, fly ash is widely recognized as a hazardous by-product, and when it is disposed of inappropriately, it will adversely affect the environment and ecology. Moreover, landfill occupation will increase [23].

In recent times, efforts have been pushed out to utilise fly ash in green and more efficient applications. Fly ash can be utilised as a base material in geopolymer cement to reduce waste and increase sustainability, rather than storing or disposing of it. However, geopolymer cement made from fly ash using ambient temperature curing exhibited unsatisfactory compressive strength, prompting researchers to explore heat curing methods (between 40 and 90 °C) as an alternative to improve the strength [24–28]. This phenomenon could be attributed to the slower reaction kinetics at ambient temperatures. Geopolymerisation, the highly exothermic chemical process that forms the geopolymeric structure, requires heat to drive the reaction forward. Lower temperatures may reduce the reaction rate, resulting in slower development of geopolymeric bonds and lower compressive strength [29,30]. Additionally, the class of FA used in geopolymer production can play a role in the compressive strength of the final product. FA is classified based on its chemical and physical properties. Class F fly ash, high in calcium and low in silica, generally exhibits lower reactivity than Class C fly ash, which has higher silica content [31]. This difference in reactivity affects the geopolymerisation process and impacts the strength of the geopolymer [32].

As a result, fly ash-based geopolymer cement using a heat curing method limits its use to precast applications. It negatively impacts the cost and climate change mitigation efforts associated with geopolymer cement acceptance [26]. Additionally, adopting heat curing in fly ash-based geopolymer cement causes rapid moisture loss, leading to drying shrinkage that can trigger tensile and shear stresses, ultimately forming cracks [33]. If ambient curing conditions can be achieved, geopolymer cement can be utilised onsite during construction, resulting in a more cost-effective and energy-efficient product than the heat curing process. Furthermore, this would enable greater flexibility in the use of geopolymer cement, providing a more versatile and eco-friendly option for the building sector. Regarding the novelty of this work, many scholars focused their studies on enhancing the mechanical strength of FA-based geopolymer cement utilising ambient temperature curing by incorporating various additives, including slag [34], OPC [35,36], alccofine [37], nano-silica [38], RHA [39], volcanic ash [40], and MK [41]. However, studies on using other potential precursors for geopolymer cement, such as silica and alumina-rich teff straw ash from teff used as a cereal in Ethiopia, are limited compared to other precursors [42].

Teff straw is an agricultural residue not valued commercially apart from being used as mud composite for rural house construction, as animal fodder, or disposed of through open-air burning. Ethiopia's annual yield of teff straw is predicted to reach 15.5 million tonnes per year [43]. However, more than two million tonnes of this valuable resource are discarded as waste and dumped in landfills, causing environmental pollution and decreasing the available land area for use [44]. Recently, researchers used teff straw for a variety of applications, including preparing activated carbon to remove heavy metals [43,45,46], production of bio-methane [44], synthesis of bio-silica [47], and using it as a natural fibre to improve the performance of concrete [48]. Teff straw ash (TSA) is a pozzolan that can be manufactured by calcinating teff straw at elevated temperatures ranging between 600 and 900 °C and can be utilised as an additional material in cement to enhance the mechanical strength of mortar [42].

The available literature shows no published research utilising TSA as source material for preparing FA-TSA blended geopolymer mortar. Therefore, this research explores the possibilities and viability of partially replacing FA with TSA in preparing FA-TSA-based geopolymer mortars using ambient temperature curing. The findings and conclusions presented here will contribute to a deeper understanding of utilising TSA in developing geopolymer cement technology. Moreover, this approach has the potential to be a valuable technique for applications that involve utilising agricultural wastes in the area of geopolymer cement technology.

2. Research significance

The current study was done to develop an ambient cured fly ash-teff straw ash-based geopolymer mortar for practical utilization in the construction industry. The research in this study was significant in multiple ways. Firstly, it addresses the need to reduce environmental costs associated with cement production. Geopolymer mortar, made from teff straw ash and fly ash, offers a sustainable approach that can lower production costs, CO_2 emissions, energy consumption, and natural resource usage, leading to a cleaner environment. This highlights the potential of geopolymer cement as an eco-friendly alternative to traditional Portland cement, with significant environmental benefits.

Secondly, the study introduces a novel technique for developing ambient-cured geopolymer mortar with comparable strength to high-temperature curing. It has practical applications in the field and extends the limitations of current heat-curing processes, making it more convenient for onsite constructions. This increases the commercial viability of geopolymers as a building material, reducing energy requirements and costs while maintaining strength. Moreover, using TSA in geopolymer technology can pave the way for further research and development of environmentally friendly products.

Furthermore, the study's results significantly affect the socio-economic aspects of utilising TSA as a source material for geopolymer cement. This could boost farmers' income, create employment opportunities, enhance the environment, and promote sustainable economic development. Overall, this study holds promise for advancing sustainable cement production, promoting innovative construction practices, and benefiting both the environment and local communities.

3. Materials and methods

3.1. Material acquisition and preparations

This study utilised various materials, including TSA, FA, river sand, an alkaline solution of sodium silicate and sodium hydroxide, as shown in Fig. 1, and tap water. Fly ash was sourced from India, while teff straw, shown in Fig. 1 (a), was obtained from Motta in the Amhara region of northern Ethiopia. To produce the ash, teff straw was incinerated in a muffle oven for 6 h at a precisely controlled temperature of 750 °C. To achieve the desired particle size for the TSA, the ash from the teff straw combustion was filtered through a 75 μm mesh to exclude oversized agglomeration of ash particles and any residual carbonaceous materials. The sodium hydroxide solution required for this study was prepared using tap water.

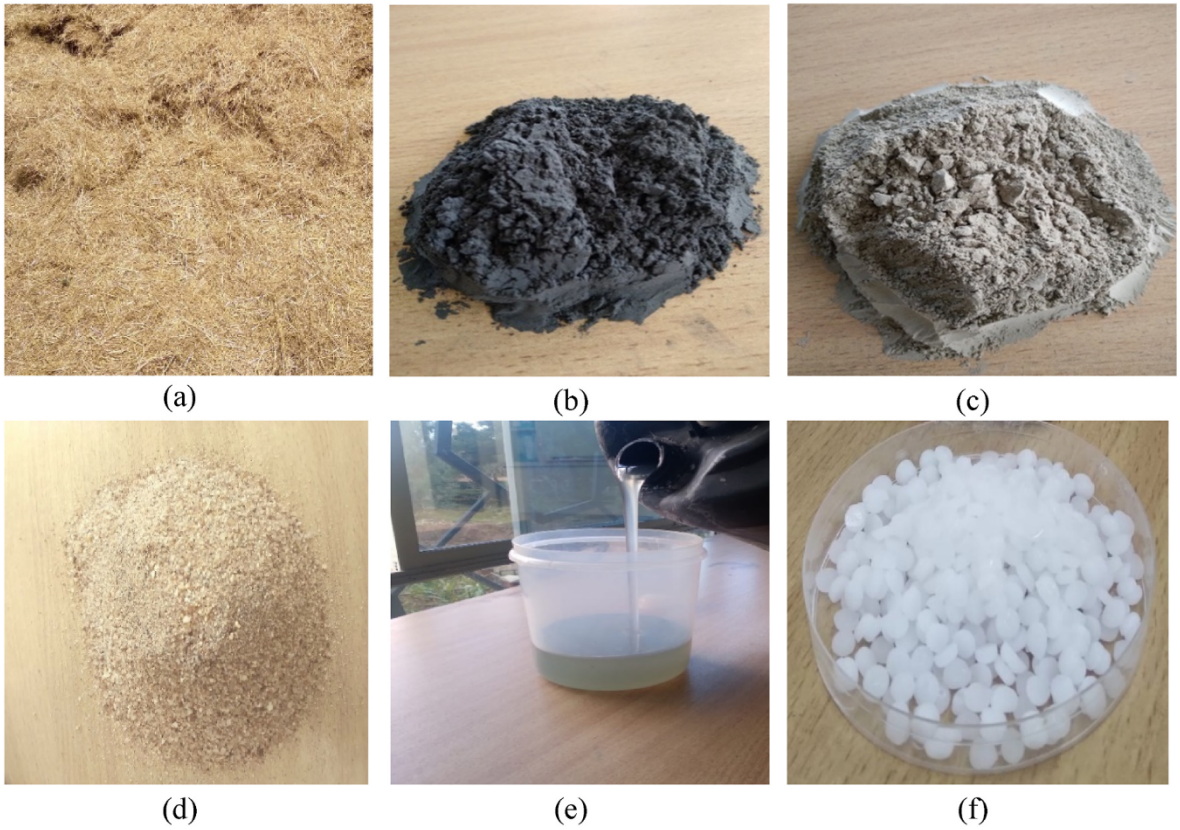

Fig. 1. (a) Teff straw, (b) TSA, (c) FA, (d) sand, (e) Na_2SiO_3 solution, and (f) NaOH pellets.

Additionally, the tap water was utilised to wash the river sand and blend the FA-TSA-based geopolymer mortar. The river sand, which had an aggregate size not exceeding 4.75 mm, was supplied from Meru, a town in eastern Kenya. The sand was prepared in air-dry conditions to ensure the desired moisture level. Initially, it was thoroughly rinsed with tap water and then oven-dried at 110 °C for 24 h before mixing.

A sodium silicate and sodium hydroxide solution were employed as an alkaline activator for preparing FA-TSA-based geopolymer mortar. The sodium silicate (Na_2SiO_3) was procured from Euro Industrial Chemicals in Nairobi, Kenya. Na_2SiO_3 was in solution form with Na_2O: SiO_2 ratio of 1:2.10. The Sodium hydroxide (NaOH) pellets manufactured by Griffchem Fine Chemicals were purchased from Science Lab Company in Nairobi, Kenya. Tap water was used to dissolve NaOH pellets to prepare a 14 M sodium hydroxide solution. To prepare a 14 M NaOH solution, 560 g of NaOH pellets were added to 500 ml of water and stirred slowly until the pellets were dissolved entirely. The resulting solution was allowed to cool and then topped with water to make 1000 ml of NaOH solution. After measuring the weight of the solution, the 560 g pellets were subtracted from it to get the weight of the water required to produce a 14 M solution. This helped in the calculation of the percentage of NaOH solids. The NaOH solution was allowed to cool for 24 h.

3.2. Methods

3.2.1. Properties of TSA, FA, and sand

The Mines and Geological Laboratories, located in Nairobi, Kenya, were utilised to conduct X-ray fluorescence to identify the TSA and FA chemical constituents. The physical properties, which included specific gravity, fineness, and particle size analysis of TSA and FA, were also analysed in conformity with the relevant standards specified by ASTM-C188 [49], ASTM-C311 [50], and ASTM-D422 [51] respectively. Microstructural analysis using scanning electron microscopy (SEM) was used to characterise the morphology of TSA and FA, whereas X-ray diffraction (XRD) analysis was conducted at Adama Science and Technology University laboratory in Ethiopia to examine their crystalline index and mineralogical phases in their dry form. The properties related to TSA and FA's physical and chemical characteristics were then compared with provisions given in ASTM-C618 [52]. The physical properties of sand, specifically the specific gravity and water absorption, were assessed using ASTM-C128 [53], while fineness modulus and particle size analysis of sand were evaluated following ASTM-C136 [54], and their properties were then compared with ASTM-C33 [55] provisions.

3.2.2. Mix proportioning

This study utilised various combinations of TSA and FA in geopolymer mortar mixes. Table 1 displays the specific proportions of the blended FA-TSA geopolymer mortars, which replaced FA with TSA at 5%, 10%, and 15% of the total binder. To label the various mixtures utilised in this study, two control mixes were prepared - CA and CE - which used FA exclusively as a binder for ambient and elevated curing, respectively. Additionally, three experimental blends were produced - 5TSA, 10TSA, and 15TSA - which replaced FA with TSA at ratios of 5%, 10%, and 15% of the total binder weight, respectively. The geopolymer mortars were prepared following the optimal formulation geopolymer

Table 1
Mix proportions in kg/m^3 of FA-TSA-based geopolymer mortar.

Mix. No.	FA	TSA	Sand	Na_2SiO_3	NaOH	Extra water
CE	714.286	–	1428.571	255.102	102.041	40.186
CA	714.286	–	1428.571	255.102	102.041	40.186
5TSA	678.571	35.714	1428.571	255.102	102.041	40.186
10TSA	642.857	71.429	1428.571	255.102	102.041	40.186
15TSA	607.143	107.143	1428.571	255.102	102.041	40.186

constituted from the literature [56,57], which consisted of the following ratios: alkaline activator solution to fly ash (0.5), fine aggregate to fly ash (2.0), water to solids (0.26), Na_2SiO_3 to NaOH (2.5), and molarity of NaOH (14 M). The additional water required to achieve saturated surface dry condition for the sand was added to the mix proportions.

3.2.3. Mixing, casting and curing

A separate mixing process was used in this study, which starts by mixing source materials with NaOH solution to dissolve the aluminium and silicon present in the raw material and then adding Na_2SiO_3 solution to enhance the binding capacity, leading to higher strength compared to other production procedures [58]. To begin the process, fly ash exclusively or fly ash in combination with TSA was blended with sand in a mixer for 3 min. Then, a pre-prepared solution of NaOH was slowly added to the dry mixture, and wet mixing was continued for three more minutes. Afterwards, a solution of Na_2SiO_3 was added to the wet mix, which was blended for an additional 5 min until it was completely uniform. Finally, the resulting mixture was poured into various standard testing moulds.

To assess the compressive, flexural, and direct tensile strengths, the fresh mixtures were poured into moulds with dimensions of 50 mm × 50 mm x 50 mm for cubes, 40 mm × 40 mm x 160 mm for prisms, and 25 mm × 25 mm in a mid-cross section for dog bone-shaped moulds, respectively. Afterwards, the samples were placed on a vibrating table and vibrated for 10 s to eliminate air voids. Then a thin plastic sheet was then utilised to shield the moulded samples from evaporation. The specimens were then placed for curing at ambient temperature (20 ± 5 °C) and activation temperature (using an oven at 75 °C for 24 h). After the curing process, the moulds containing CE were taken out of the oven and allowed to cool down naturally at room temperature before being demoulded. The sealed CA, CE, 5TSA, 10TSA, and 15TSA samples were then maintained under normal environmental conditions until the samples reached the testing ages of 7, 14, and 28 days, respectively.

3.2.4. Testing

The flowability of freshly made geopolymer mortars was assessed by employing the flow table method specified in the ASTM C1437-07 standard [59]. The required flow diameter of 110 ± 5% was established as a benchmark to ensure the flow of FA-TSA-based geopolymer mortar. The compressive, flexural, and direct tensile strengths of geopolymer mortar were examined after 7, 14, and 28 days of curing as per ASTM standards C109/C109M − 08 [60], C348-08 [61], and C307-03 [62], respectively. The test was performed on three samples, and the results were averaged. The fragments from geopolymer mortar samples subjected to compressive strength at 28 days were selected for SEM analysis to investigate the microstructure. Finely divided samples for geopolymer specimens tested for compressive strength after 28 days filtering through a 75 μm mesh were used for XRD to investigate the mineralogical phases of FA-TSA-based geopolymer mortar.

4. Results and discussion

4.1. Characterisation of source materials

Table 2 displays the physical characteristics of both FA and TSA, while their respective particle size distributions are illustrated in Fig. 2. TSA particles have a finer particle size distribution than FA particles, which reduces voids and thus improves the microstructure as well as the mechanical strength of geopolymer mortar. The degree of fineness of TSA is a critical factor that can substantially impact the flowability of the blended FA-TSA geopolymer mixes due to increased water demand. The SEM images in Fig. 3 show that FA particles are spherical-shaped balls with broken Cenospheres, whereas TSA particles are flaky and angular-type irregular shapes. The SEM analysis revealed that the TSA surfaces possess a loose binding, which enhances its amorphous and reactive characteristics. Additionally, numerous residual pores were evident throughout the ash samples, demonstrating the silica's high porosity and active nature. Table 3 shows the chemical constituents of TSA and FA. The compositions of SiO_2, Al_2O_3, and Fe_2O_3 compounds in the TSA were 72.01%, which can be classified as class N, while in the FA, the composition was 84.65%, and CaO was less than 10%, which can be classified as class F pozzolanic materials as per ASTM C618 [52]. As shown in Fig. 4, the major mineralogical phases of FA were mullite, quartz, magnetite, and hematite, whereas the major mineralogical phases of TSA were quartz, magnetite, and hematite. The crystalline indexes of FA and TSA were 37.75% and 20.04%, respectively.

Table 2
Physical properties of teff straw ash and fly ash.

Physical properties	TSA	FA	ASTM C 618
The amount retained on 45 μm sieve (fineness)	4%	7%	Max (34%)
Median particle size (mm), d_{50}	0.007	0.008	–
Specific gravity	2.0	2.5	–

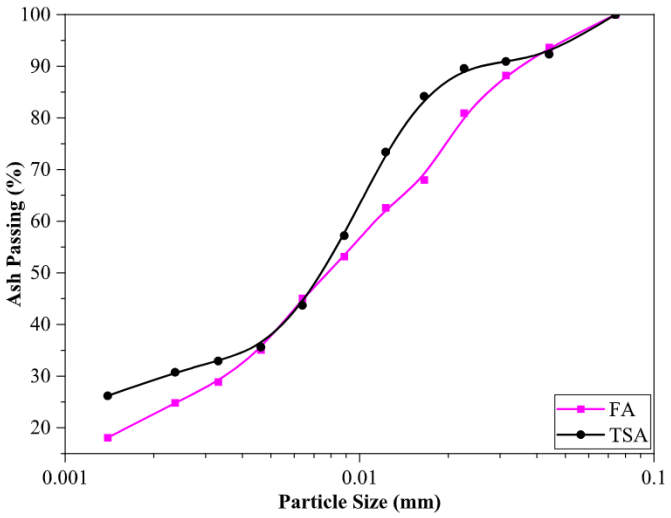

Fig. 2. Particle size analysis of teff straw ash and fly ash.

4.2. Characterisation of alkaline activator and sand

The properties of NaOH pellets and Na_2SiO_3 solution are shown in Table 4. The particle size analysis of sand used for the production of FA-TSA-based geopolymer mortars, as shown in Fig. 5, was found to be within the recommended envelope, and the fineness modulus was found to be 2.52, which is within the range of 2.2–2.6 as per ASTM C33 [55]. Additionally, sand's water absorption and specific gravity were 2.81% and 2.51, respectively.

4.3. Fresh properties of FA-TSA-based geopolymer mortar

Fig. 6 displays the flow values of FA-TSA-based geopolymer mortars, which were tested in accordance with ASTM C1437-20 standards. The results indicate that the flow values of the geopolymer mortar were within the acceptable range of 110 ± 5%. However, when TSA was incorporated into the formulation of the geopolymer mortar at 5%, 10%, and 15%, the flow values decreased by 1.8%, 3.5%, and 6%, respectively. These findings suggest that as the percentage of TSA in the mixture increased, the flowability of the geopolymer mortars consistently decreased. This can be linked to the shape and texture of the TSA particles. It has been reported that the flow of geopolymers can be significantly influenced by several factors, including the particle size of the source material, amount and type of alkaline activator used, molarity of NaOH, water-to-binder ratio, and the properties of the

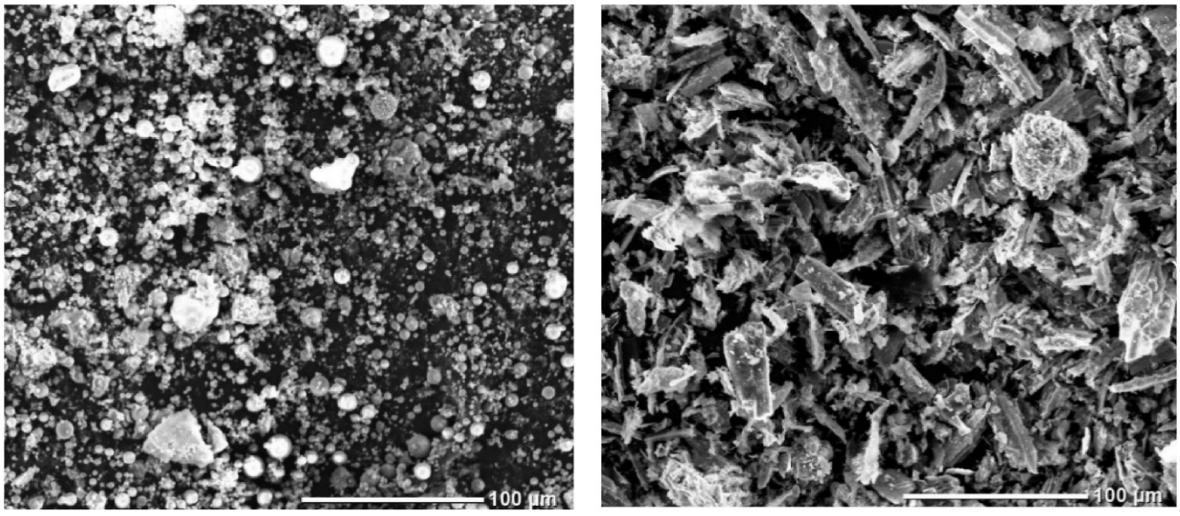

Fig. 3. SEM images of (a) FA and (b) TSA.

Table 3
Chemical constituent of teff straw ash and fly ash using XRF (%).

Chemical Composition	TSA	FA	ASTM C 618
SiO_2	63.20	55.87	–
Al_2O_3	5.37	22.66	–
Fe_2O_3	3.44	6.12	–
CaO	4.08	6.50	Max (10%)
MgO	3.34	5.19	–
K_2O	12.20	–	–
SO_3	–	0.36	Max (5%)
$SiO_2 + Al_2O_3 + Fe_2O_3$	72.01	84.65	Min (70%)
Loss on ignition	4.33	1.75	Max (6%)
Moisture content	1.47	0.95	Max (3%)

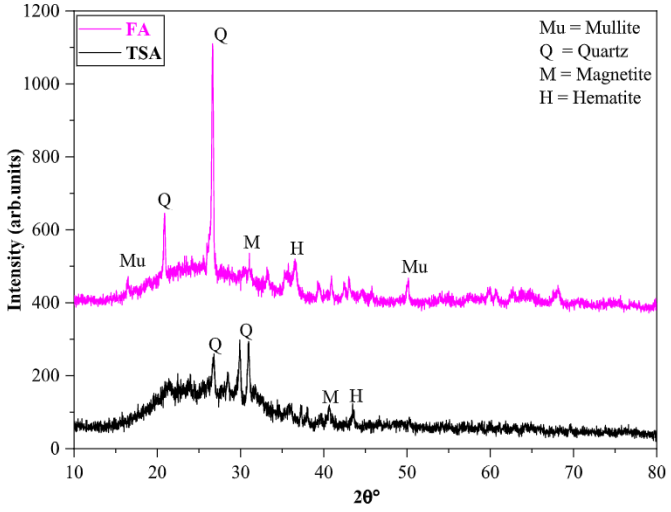

Fig. 4. XRD patterns of TSA and FA.

Table 4
Properties of the NaOH pellet and Na_2SiO_3 solution.

Compound	Specific gravity	Na_2O (%)	SiO_2 (%)	Total solids (%)	Purity (%)
Na_2SiO_3	1.53	14.07	29.55	43.62	–
NaOH	1.34	–	–	41.70	98

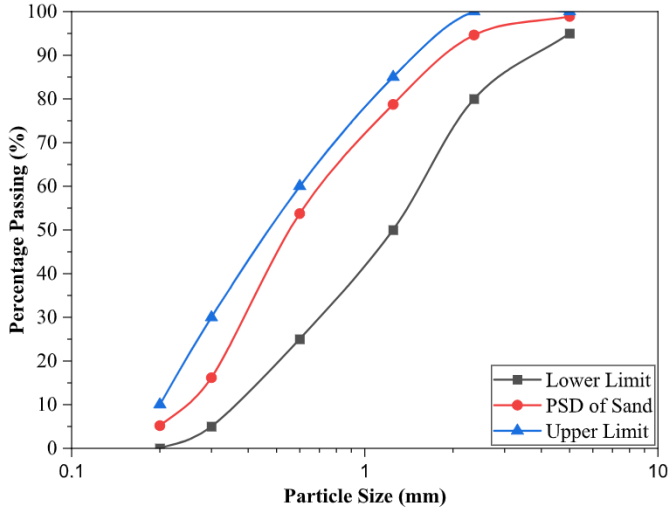

Fig. 5. Particle size analysis of river sand.

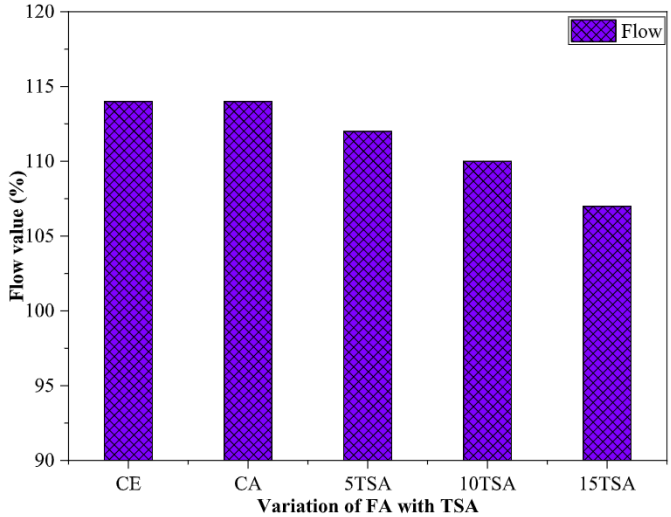

Fig. 6. Influence of TSA variations on the workability of geopolymer mortar.

ingredients used in the mix design [63].

The angular and flaky shape, as well as the rough surface texture and loose binding of the TSA particles, lead to higher water absorption and an increase in water demand for the FA-TSA geopolymer mortar [64]. Furthermore, since TSA is finer than FA, as illustrated in Fig. 2, which increases the water demand and thus reduces the flowability of freshly blended geopolymer mortar containing FA-TSA [65]. Additionally, the high reactivity of TSA can also reduce the flowability of the mix.

4.4. Mechanical performance FA-TSA-based geopolymer mortar

4.4.1. Compressive strength

The findings illustrated in Fig. 7 suggest that higher TSA content levels significantly enhanced the mortar's strength under compression, even during the initial curing stages. For instance, the compressive strengths after 7 days for CE, CA, 5TSA, 10TSA, and 15TSA mixes were 48.71, 16.29, 21.76, 25.45, and 22.56 MPa, respectively. At the age of 7 days, CE had higher compressive strength than CA and specimens containing TSA. This indicates that the geopolymerisation process for CE was almost completed due to the heat curing that can help to overcome the activation energy barrier, increase the reaction rate, facilitate the reaction with water molecules, and promote the formation of strong bonds between the reactants [66]. Further, an observation confirmed by the CE showed a slight improvement in compressive strength at 28 days. Additionally, the results revealed that TSA specimens had higher compressive strength than the CA, which indicates the possibility of increased geopolymerisation with TSA.

After 14 days, it was observed that the compressive strength of both the CA and TSA specimens remained lower than that of the CE specimens. This is because the low CaO content in the FA and TSA may limit the availability of calcium ions (Ca^{2+}) to form polymeric chains, leading to slower geopolymerisation and, subsequently, the strength development of geopolymer mortar. Ca^{2+} ions are crucial in forming calcium silicate hydrate (C–S–H) gel, which contributes to the strength of geopolymer materials. With reduced Ca^{2+} availability, the geopolymerisation process may be less efficient, resulting in lower early strength in geopolymer mortar [35,67,68]. The 14-day compressive strength of the CE showed an improvement of 1.04% over its 7-day strength and a remarkable 49.37% over the CA mixture. Furthermore, the geopolymer mortar made with 5TSA, 10TSA, and 15TSA continued to develop higher compressive strengths by 18%, 49%, and 35%, respectively, compared to the CA mixture, indicating that the geopolymerisation reaction is continuously extending in the presence of TSA at 5, 10 and 15% of the binder.

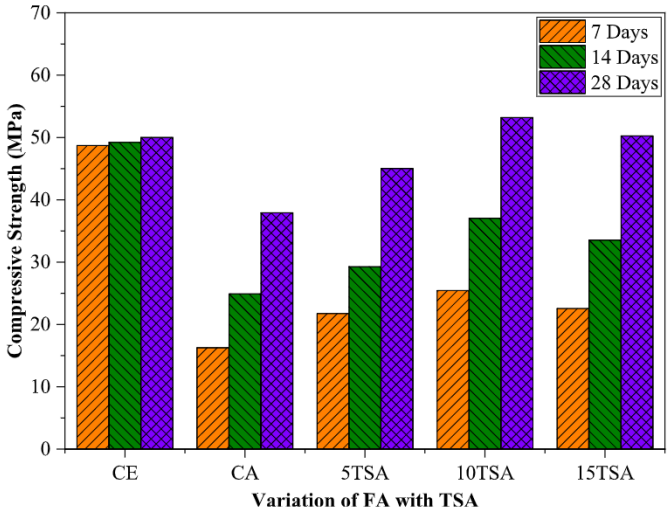

Fig. 7. Influence of TSA variations on the compressive strength of mortar specimens.

At 28 days, the compressive strength of the CE remained higher than that of the CA and 5TSA but was comparable to that of the 15TSA specimen. The 5TSA, 10TSA, and 15TSA specimens achieved 19%, 40%, and 33% higher compressive strengths than the CA mixture, respectively. The experimental results revealed that the 10TSA mixture exhibited a peak compressive strength of 53.22 MPa at 28 days, surpassing the compressive strengths of both the CE (50.02 MPa) and CA (37.92 MPa) mixtures. This suggests that the 10TSA blend could be a good choice for achieving higher compressive strengths of geopolymer mortar at ambient curing temperatures. The findings showed that increasing the TSA content to 15% in the geopolymer mortar resulted in a 5.5% reduction in compressive strength compared to the 10% TSA content. This decrease in compressive strength can be attributed to the higher alkaline activator solution demand associated with the increased TSA content. The increased demand for an alkaline activator solution hindered the proper mixing of geopolymer ingredients and led to incomplete activation of the precursor, resulting in reduced compressive strength compared to the 10% TSA mixture.

According to the principal outcomes of this investigation, increasing the quantity of TSA led to a remarkable enhancement of the compressive strength of the composite. In addition, it enabled the successful curing of FA-TSA-based geopolymer mortar under ambient temperature conditions. Previous studies [69] found that the morphology of the source materials had a substantial effect on the mechanical performance following activation. The results depicted in Fig. 2 suggest that TSA particles with smaller size and higher fineness offer an increased surface area for interaction with alkaline solutions, leading to a more favourable mechanical performance of the FA-TSA-based geopolymer mortar. Further, to attain charge balance in the geopolymer matrix, supplementary cations such as Na^+, K^+, and Ca^{2+} were utilised, as highlighted in previous research [15]. As indicated in Table 3, TSA contains a K_2O content of 12.2%, which can have a positive impact on the geopolymerisation reaction by serving as a supplemental source of cations (K^+) and helping in the charge balance of the resulting geopolymer structure, as reported by other studies [70].

Moreover, TSA is rich in silica, as shown in Table 3, which results in an improved aluminium integration within the geopolymer network structure. Additionally, during the initial reaction stage, silica facilitates the formation of aluminium and silicon nuclei from unreacted particles in the source material [71]. Furthermore, as shown in Fig. 4, teff straw ash was more highly amorphous than fly ash. During alkali activation, amorphous phases in the source materials dissolve faster than crystalline phases, resulting in a more stable and strong geopolymer binder [72,73]. Moreover, the addition of TSA favours the formation of other mineralogical phases, which helps in improving the compressive strengths of geopolymer mortar, as discussed further in Section 4.5.1.

4.4.2. Flexural strength

Fig. 8 illustrates the flexural strength outcomes of the hardened geopolymer mortar samples after 7, 14, and 28 days. The CE specimens displayed a higher flexural strength than CA for all the test ages. In general, the 10TSA combination displayed the strongest flexural strength across all testing periods. However, the combinations of 5TSA and 15TSA demonstrated interesting flexural strength development, while mixture CA showed the weakest flexural strength at all testing intervals. The flexural strengths of geopolymer mortar samples comprising 5TSA, 10TSA, and 15TSA were approximately 44%, 74%, and 55% greater than that of mixture CA after 7 days, respectively. Moreover, the geopolymer samples with 10TSA sustained a significant flexural strength improvement of nearly 63% more than CA after 14 days. In contrast, the geopolymer mortars containing 5TSA and 15TSA demonstrated strength increases of only 39% and 48% higher than the CA, respectively.

At 28 days, the geopolymer mortars containing 5TSA, 10TSA, and 15TSA exhibited flexural strengths comparable to CE and even outperformed it by 0.5%, 15%, and 5%, respectively. Furthermore, the

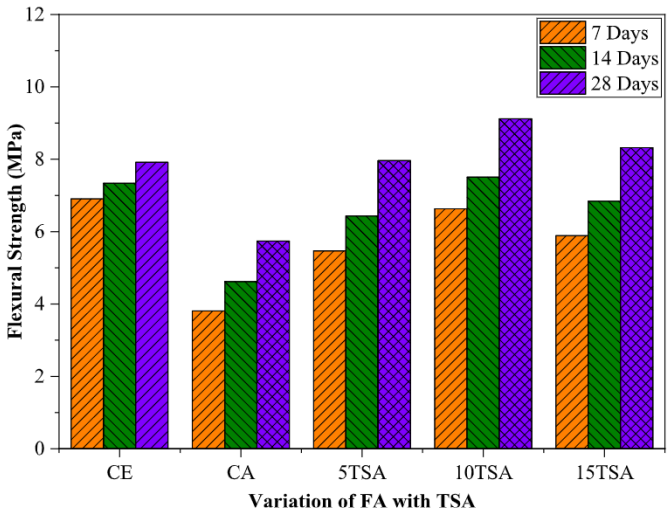

Fig. 8. Influence of TSA variations on the flexural strength of mortar specimens.

flexural strength of the geopolymer mortars containing TSA also showed significantly higher strengths than CA, with increases of 37%, 59%, and 45% for 5TSA, 10TSA, and 15TSA, respectively. The reason behind this is that the inclusion of TSA resulted in rapid and high reaction rates, leading to a high concentration of geopolymer products, such as N-A-S-H and C-A-S-H gel, which enhanced the strength of the 5TSA, 10TSA, and 15TSA mixtures. According to previous findings, the high concentration of geopolymer products fills the microscopic pores and creates more consolidated binder frameworks as well as stronger binder-aggregate interfacial regions [70]. As a result, the FA-TSA-based geopolymer mortars displayed a greater capacity to resist bending forces when exposed to flexural stresses.

The relationship between flexural strength and compressive strength of FA-TSA-based geopolymer mortar is depicted in Fig. 9, showing a strong positive linear relationship with a correlation of determination (R^2) value of 0.9033. This indicates a high degree of correlation between the two properties, suggesting that an increase in flexural strength is associated with an increase in compressive strength and vice versa. The findings demonstrate a direct relationship between these two strengths in geopolymer mortar, with flexural strength values showing an upward trend as compressive strength values increase. These results are consistent with previous studies [74] that have reported similar relationships between flexural strength and compressive strength in slaked lime-based alkali-activated mortars.

4.4.3. Tensile strength

The results in Fig. 10 demonstrate the direct tensile strength of FA-TSA-based geopolymer blends with different levels of TSA for 7, 14, and 28 days. The analysis revealed that an increase in TSA significantly impacted the direct tensile strength at all curing stages. The CE mixture exhibited a higher tensile strength at 7 and 14 days than the CA, 5TSA, 10TSA, and 15TSA mixtures. Moreover, at 28 days, the CE mixture had a higher tensile strength than the CA mixture. Furthermore, the samples containing 10% TSA had the highest direct tensile strength after 28 days of curing, approximately 18% and 30% higher than the CE and CA mixtures, respectively. The tensile strength for the 5TSA mixture was higher than for the CA mixture and comparable with the CE mixture, while the tensile strength for 15TSA was less than the tensile strength for 10TSA but higher than CE, CA, and 5TSA at 28 days. The CE mixture exhibited a better tensile strength at 7 days due to complete geopolymerisation, while the 10TSA and 15TSA mixtures exhibited higher tensile strength at 28 days due to increased aggregate-paste bond strength and microstructure refinement. Overall, the results suggest that adding TSA can significantly improve the direct tensile strength of FA-based geopolymer blends, with a TSA content of 10%.

4.5. Microstructure

4.5.1. X-ray diffraction analysis

Fig. 11 illustrates the XRD examination of FA-TSA-based geopolymer mortars after 28 days. The broad peaks detected within the 20° to 53.3° on the 2θ scale indicate a geopolymerisation reaction, resulting in the geopolymer product development. Moreover, the peaks suggest the presence of a dominant crystalline phase alongside a minor amorphous phase in the geopolymer mortar. In addition, both mixtures CA and CE demonstrated the presence of partially crystalline phases previously identified in the XRD analysis of FA (Fig. 4), along with a new phase composed of albite, analcim, and anorthite, which emerged from the geopolymerisation reaction. The N-A-S-H gel family, specifically the partially crystalline phase of albite, is recognized as a geopolymeric product of sodium-polysialate, as mentioned in previous studies [75, 76].

After 28 days, the XRD pattern of the 5TSA, 10TSA, and 15TSA mixtures exhibited substantially higher peak formations than the CE and CA mixtures. Significant major peaks suggest a greater dissolution of precursors in the alkali-activated FA-TSA-based geopolymer mortar,

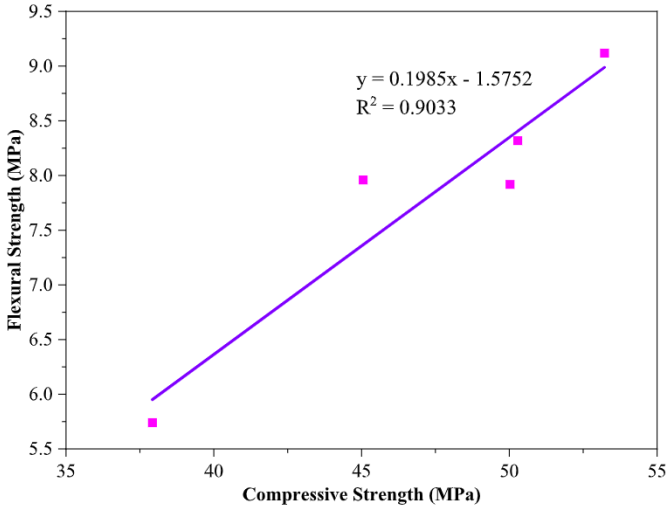

Fig. 9. Relationship between compressive and flexural strength of geopolymer mortar.

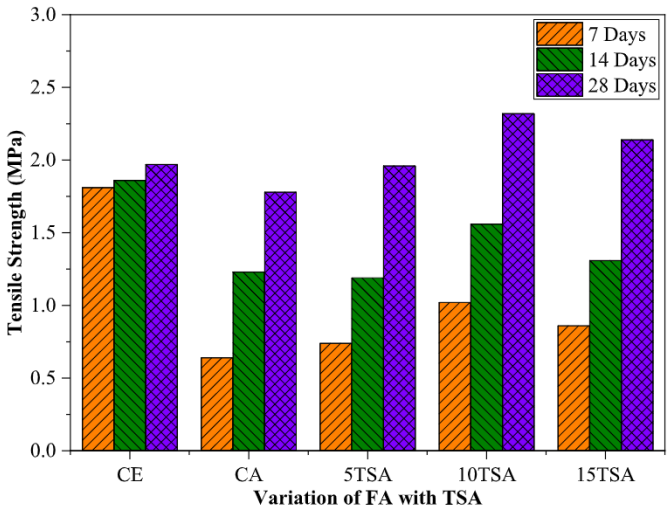

Fig. 10. Influence of TSA variation on the direct tensile strength of mortar specimens.

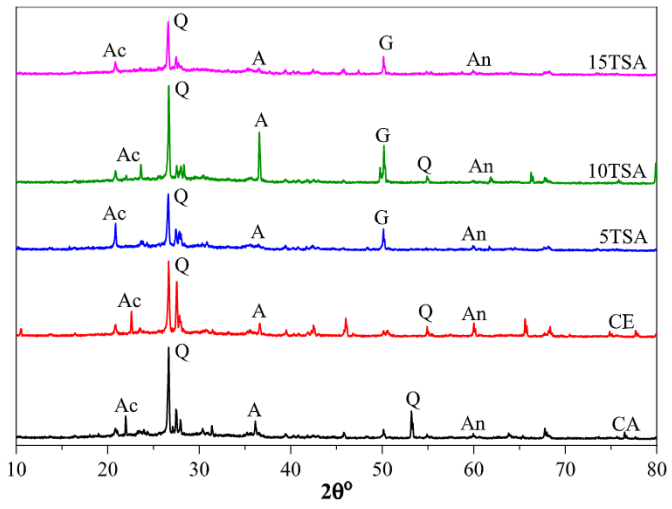

Fig. 11. XRD patterns of FA-TSA-based geopolymer mortars after 28 days. [Note: Ac: Analcim, Q: Quartz, A: Albite, G: Gismondine, An: Anorthite].

indicating a high degree of geopolymerisation [77]. Moreover, geopolymeric products, such as aluminium silicate and amorphous N-A-S-H gel, form a three-dimensional amorphous gel-like structure that significantly enhances cohesion and effectively prevents crack propagation [78]. This notable improvement in the strength of the geopolymeric material was observed in the specimens with 5TSA, 10TSA, and 15TSA content. Moreover, it can be noted from Fig. 11 that there was an increase in analcim concentration in the 10TSA mixture.

In addition, a novel semi-crystalline phase of gismondine was detected in the 5TSA, 10TSA, and 15TSA blend, along with previously identified mineralogical phases such as analcim, anorthite, albite, and quartz from CA and CE samples. According to reports [59], the recently produced gismondine phase is categorised as a C-A-S-H gel and can serve as sites for nucleation that promote the formation of extra geopolymer bonds, resulting in a denser and greater interlocked microstructure. Recent studies have shown that in this gel, a new phase of Al^{3+} enters the C–S–H structure [79]. This partially substitutes Si^{4+} with Al^{3+} in the silicon-oxygen tetrahedron, while the remaining Al^{3+} ions enter the C–S–H layer. This intriguing phenomenon leads to the formation of an electrically neutral structure and a significant increase in the degree of polymerization of the silicon-oxygen tetrahedron [80].

Additionally, C-A-S-H aids in the early-age strength development of geopolymers since it forms more rapidly than N-A-S-H [81]. Consequently, this enhances the mechanical performance of FA-TSA-based geopolymer mortar, including its compressive, flexural, and direct tensile strengths. This phase probably resulted from the chemical interaction of ionic constituents that originated from the dissolution of TSA and FA as a precursor.

4.5.2. Scanning electron microscopy analysis

Fig. 12 presents the SEM image of FA-TSA-based geopolymer mortar after 28 days of curing. The results obtained from the CA samples revealed the presence of large spheres of unreacted fly ash, leading to void spaces and a less dense structure in the geopolymer mortar. These voids resulted from the incomplete dissolution of fly ash during the fresh mixing of geopolymer mortar. In contrast, the CE samples showed a marked improvement in homogeneity and density of the gel matrices compared to the CA samples. Moreover, the portion of unreacted or partially reacted fly ash microspheres in the CE mixture was comparatively lower than in the CA mix. The slower dissolution rate of fly ash affected the geopolymerisation process, resulting in higher porosity in the CA sample.

Furthermore, unreacted fly ash particles and free water's evaporation during the curing and aging processes may have played a role in the initiation and propagation of microcracks [75]. The formation and propagation of these microcracks could adversely affect the mechanical properties of the FA-TSA-based geopolymer mortar. The unreacted particles weaken the geopolymer structure. Therefore, the insufficient dissolution of fly ash and the resulting unreacted fly ash particles can be considered a significant contributing factor to the reduction in mechanical properties observed in both CA and CE samples [82].

Adding TSA to the overall binder content resulted in significant improvements in the microstructure of geopolymer mortars compared to the control mixes (CA and CE). After 28 days, the microstructure of the 5TSA and 15TSA mixtures exhibited a marked enhancement in the uniformity and compactness of the gel structure than those of CA and CE mixtures. Furthermore, the concentration of unreacted or partially reacted fly ash particles was relatively lower in the 5TSA and 15TSA mixtures compared to CA and CE. Similarly, the microstructure of the 10TSA mixture after 28 days demonstrated a notable improvement in the uniformity and compactness of the gel structure compared to that of the 5TSA and 15TSA mix. Additionally, in the 10TSA mixture, pore spaces and unreacted or partially reacted fly ash particles were almost invisible in the microstructure of the geopolymer mortar, in contrast to CA, CE, 5TSA, and 15TSA mixtures.

During the geopolymerisation process, the chemical reaction between the alkaline solution and aluminosilicate materials results in the dissolution of fly ash and teff straw ash. This reaction leads to the formation of geopolymeric gels that effectively fill the voids and interstitial spaces within the geopolymer mortar [83]. As a result, the microstructure of the geopolymer mortar with a 10TSA mixture becomes more uniform and compact, with the geopolymeric gels acting as a binder that binds the particles together. This process creates a solid matrix with enhanced uniformity and compactness of the 10TSA mixture.

The 10TSA mixture's compacted microstructure, as shown in Fig. 12 (d), allowed it to achieve the highest mechanical strength after 28 days compared to the CA, CE, 5TSA, and 15TSA mixtures. This indicates that when 10% TSA was added to the mixture, fly ash and teff straw ash particles dissolved more rapidly in the highly alkaline medium than the fly ash particles in CA and CE. As a result, the reaction products played a significant role in enhancing the refinement of the microstructure and preventing the formation of microcracks, leading to minimal microcrack formation and compact reacted geopolymer structures in the 10TSA mixture [84]. Consequently, the 10TSA mixture exhibited slightly higher early strength than the control mixes after 28 days, as discussed in section 4.4.

5. Conclusions

Based on the findings presented in this study, it can be concluded as described here.

- When TSA was used as a partial substitute for FA, the workability of the blended mixtures decreased.
- By partially substituting FA with TSA, it is possible to manufacture hardened geopolymer materials without the requirement of heat curing. The best 28-day compressive strength was attained with the 10TSA mixture, which had a strength of 53.22 MPa when cured at ambient temperature. This strength was even greater than that of CE, which was cured at a higher temperature and had a compressive strength of 50.02 MPa, and that of CA, which achieved a compressive strength of 37.92 MPa using ambient temperature curing.
- The 10TSA mixture exhibited superior flexural and tensile strength performance at 28 days when cured at ambient temperature. Its flexural strength was 9.12 MPa, surpassing that of CE (7.92 MPa) and CA (5.74 MPa). Similarly, its tensile strength was 2.32 MPa, higher than that of CE (1.97 MPa) and CA (1.78 MPa).
- The influence of TSA variation on the improvement of flexural and direct tensile strengths in the curing of FA-TSA-based geopolymer

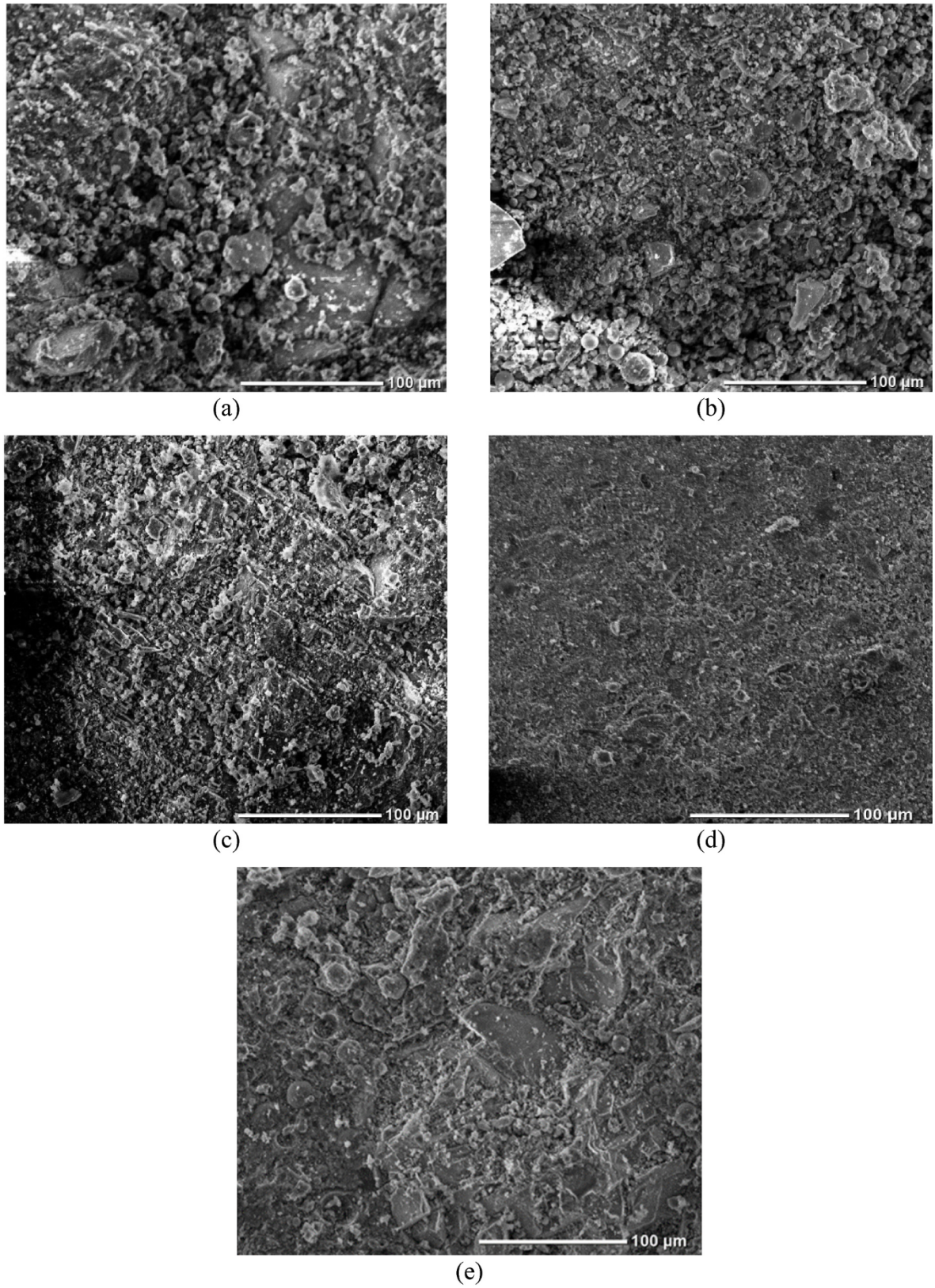

Fig. 12. SEM of mortars at 28 days (a) CA, (b) CE, (c) 5TSA, (d) 10TSA, (e) 15TSA.

mortar at ambient temperature demonstrated a similarity to the impact on the enhancement of compressive strength.

- The mineralogical phase determined by XRD demonstrated the existence of analcim, albite, quartz, and anorthite phases in the control mixes (CA and CE) after 28 days. Conversely, the geopolymer mortars that incorporated TSA exhibited the presence of alumino silicate gel and gismondine, along with quartz, albite, analcim, and anorthite phases.

- The SEM image of the 10TSA mixture indicated an enhancement in the compactness of the geopolymer matrix, with a relatively lower concentration of unreacted or partially reacted FA particles in comparison to CA and CE.

The current study concludes that the investigated geopolymer mixes with increased TSA content had significantly enhanced compressive, flexural, and tensile strengths. Furthermore, it did not require heat curing, making it a viable option for onsite applications. These findings suggest that using TSA as a substitute for FA in geopolymer cement can reduce energy consumption and environmental issues without compromising the mechanical performance of the mortar. The results, as mentioned above, can also be used as a foundation for future developments in geopolymer mortar curing using TSA at ambient temperature. Additionally, incorporating TSA into geopolymer production reduces the need for costly and ecologically-friendly disposal of TSA in landfills and protects the environment from being polluted.

6. Recommendations

The study was limited to examining the microstructural and mechanical performance of ambient cured fly ash-based geopolymer mortar using teff straw ash. As a result, the following aspects for further investigation are suggested:

- Future studies should explore the thermal performance and durability properties of FA-TSA-based geopolymers.
- To explore possibilities for product commercialisation, evaluating the economic and environmental benefits of employing teff straw ash in the preparation of geopolymers is crucial.

Credit author statement

Tajebe Bezabih Mekonen: Conceptualization, Methodology, Validation, Formal analysis, Investigation, Resources, Writing – original draft, Writing – review & editing, Visualization, Project administration, Funding acquisition. **Christopher Kanali**: Supervision, Validation, Writing – review & editing, Project administration. **Joseph Thuo**: Supervision.

Declaration of competing interest

The authors declare that they have no known competing financial interests or personal relationships that could have appeared to influence the work reported in this paper.

Data availability

Data will be made available on request.

Acknowledgement

The authors thank the Pan African University of Sciences, Technology, and Innovation (PAUSTI) for their unwavering and constructive support throughout this research study.

References

[1] C.R. Gagg, Cement and concrete as an engineering material: an historic appraisal and case study analysis, Eng. Fail. Anal. 40 (2014) 114–140, https://doi.org/10.1016/j.engfailanal. 2014.02.004.
[2] S.A. Miller, A. Horvath, P.J.M. Monteiro, Impacts of booming concrete production on water resources worldwide, Nat. Sustain. 1 (2018) 69–76, https://doi.org/10.1038/s 41893-017-0009-5, 2018 11.
[3] A. Danish, T. Ozbakkaloglu, M. Ali Mosaberpanah, M.U. Salim, M. Bayram, J. H. Yeon, K. Jafar, Sustainability benefits and commercialization challenges and strategies of geopolymer concrete: a review, J. Build. Eng. 58 (2022), 105005, https://doi.org/10.1016/J.JOBE.2022.105005.
[4] M.G. Omer Adam, D.O. Koteng, J.N. Thuo, M. Matallah, Effects of acid attack and cassava flour dosage on the interfacial transition zone thickness, durability and mechanical characteristics of high-strength (HS) concrete, Results Eng 17 (2023), 101001, https://doi.org/10.1016/J.RINENG.2023.101001.
[5] M.S. Imbabi, C. Carrigan, S. McKenna, Trends and developments in green cement and concrete technology, Int. J. Sustain. Built Environ. 1 (2012) 194–216, https://doi.org/10.1016/J.IJSBE.2013.05.001.
[6] Y.H.M. Amran, R. Alyousef, H. Alabduljabbar, M. El-Zeadani, Clean production and properties of geopolymer concrete; a review, J. Clean. Prod. 251 (2020), 119679, https://doi.org/10.1016/J.JCLEPRO.2019.119679.
[7] M.G. Khalil, F. Elgabbas, M.S. El-Feky, H. El-Shafie, Performance of geopolymer mortar cured under ambient temperature, Construct. Build. Mater. 242 (2020), 118090, https://doi.org/10.1016/J.CONBUILDMAT.2020.118090.
[8] R. Kajaste, M. Hurme, Cement industry greenhouse gas emissions – management options and abatement cost, J. Clean. Prod. 112 (2016) 4041–4052, https://doi.org/10.1016/J.JCLEPRO.2015.07.055.
[9] R. Maddalena, J.J. Roberts, A. Hamilton, Can Portland cement be replaced by low-carbon alternative materials? A study on the thermal properties and carbon emissions of innovative cements, J. Clean. Prod. 186 (2018) 933–942, https://doi.org/10.1016/J.JCLEPRO.2018.02. 138.
[10] L.N. Assi, K. Carter, E. Deaver, P. Ziehl, Review of availability of source materials for geopolymer/sustainable concrete, J. Clean. Prod. 263 (2020), 121477, https://doi.org/10.1016/J.JCLEPRO.2020.121477.
[11] A.L. Almutairi, B.A. Tayeh, A. Adesina, H.F. Isleem, A.M. Zeyad, Potential applications of geopolymer concrete in construction: a review, Case Stud. Constr. Mater. 15 (2021), e00733, https://doi.org/10.1016/J.CSCM.2021.E00733.
[12] D.K. Panesar, Supplementary cementing materials, Dev. Formul. Reinf. Concr. (2019) 55–85, https://doi.org/10.1016/B978-0-08-102616-8.00003-4.
[13] A. Mohajerani, D. Suter, T. Jeffrey-Bailey, T. Song, A. Arulrajah, S. Horpibulsuk, D. Law, Recycling waste materials in geopolymer concrete, Clean Technol. Environ. Policy 213 (2019) 493–515, https://doi.org/10.1007/S10098-018-01660-2, 21 (2019.
[14] A. Longos, A.A. Tigue, R.A. Malenab, I.J. Dollente, M.A. Promentilla, Mechanical and thermal activation of nickel-laterite mine waste as a precursor for geopolymer synthesis, Results Eng 7 (2020), 100148, https://doi.org/10.1016/J.RINENG.2020.100148.
[15] J. Davidovits, Geopolymer cement a review, Publ. Geopolymer Sci. Tech. Tech. Pap. #21, Geopolymer Inst. Libr. (2013) 1–11. w.w.w.Geopolymer.Org.
[16] B.B. Jindal, Investigations on the properties of geopolymer mortar and concrete with mineral admixtures: a review, Construct. Build. Mater. 227 (2019), 116644, https://doi.org/10.1016/J.CONBUILDMAT.2019.08.025.
[17] F. Kantarci, İ. Türkmen, E. Ekinci, Influence of various factors on properties of geopolymer paste: a comparative study, Struct. Concr. (2020) 1–17, https://doi.org/10.1002/SUCO. 201900400.
[18] M. Kaya, F. Köksal, M. Bayram, M. Nodehi, O. Gencel, T. Ozbakkaloglu, The effect of marble powder on physico-mechanical and microstructural properties of kaolin-based geopolymer pastes, Struct. Concr. (2022), https://doi.org/10.1002/SUCO.202201010.
[19] A. Nikolov, H. Nugteren, I. Rostovsky, Optimization of geopolymers based on natural zeolite clinoptilolite by calcination and use of aluminate activators, Construct. Build. Mater. 243 (2020), 118257, https://doi.org/10.1016/J.CONBUILDMAT.2020.118257.
[20] G. Mathew, B.M. Issac, Effect of molarity of sodium hydroxide on the aluminosilicate content in laterite aggregate of laterised geopolymer concrete, J. Build. Eng. 32 (2020), 101486, https://doi.org/10.1016/J.JOBE.2020.101486.
[21] Z. Tian, X. Tang, Z. Xiu, H. Zhou, Z. Xue, The mechanical properties improvement of environmentally friendly fly ash-based geopolymer mortar using bio-mineralization, J. Clean. Prod. 332 (2022) 1–9, https://doi.org/10.1016/j.jclepro.2021.130020.
[22] P. Suraneni, L. Burris, C.R. Shearer, R.D. Hooton, ASTM C618 fly ash Specification: comparison with other Specifications, Shortcomings, and solutions, ACI Mater. J. 118 (2021) 157–168, https://doi.org/10.14359/51725994.
[23] X.Y. Zhuang, L. Chen, S. Komarneni, C.H. Zhou, D.S. Tong, H.M. Yang, W.H. Yu, H. Wang, Fly ash-based geopolymer: clean production, properties and applications, J. Clean. Prod. 125 (2016) 253–267, https://doi.org/10.1016/J.JCLEPRO.2016.03.019.
[24] B.B. Jindal, Feasibility study of ambient cured geopolymer concrete -A review, Adv. Concr. Constr. 6 (2018) 387–405, https://doi.org/10.12989/ACC.2018.6.4.387.
[25] M. B.S, I.G.S. Muhd Fadhil Nurruddin, Sani Haruna, Methods of curing geopolymer concrete: a review, Int. J. Adv. Appl. Sci. 5 (2018) 31–36, https://doi.org/10.21833/ijaas. 2018.01.005.
[26] W.P. Zakka, N.H. Abdul Shukor Lim, M. Chau Khun, A scientometric review of geopolymer concrete, J. Clean. Prod. 280 (2021), 124353, https://doi.org/10.1016/J.JCLEPRO.2020.124353.
[27] P. Jitsangiam, T. Suwan, K. Pimraksa, P. Sukontasukkul, P. Chindaprasirt, Challenge of adopting relatively low strength and self-cured geopolymer for road construction application: a review and primary laboratory study, Int. J. Pavement Eng. 22 (2019) 1454–1468, https://doi.org/10.1080/10298436.2019.1696967.
[28] K. Neupane, Fly ash and GGBFS based powder-activated geopolymer binders: a viable sustainable alternative of portland cement in concrete industry, Mech. Mater. 103 (2016) 110–122, https://doi.org/10.1016/J.MECHMAT.2016.09.012.
[29] A.M. Mustafa Al Bakria, H. Kamarudin, M. Bin Hussain, I. Khairul Nizar, Y. Zarina, A.R. Rafiza, The effect of curing temperature on physical and chemical properties of geopolymers, Phys. Procedia 22 (2011) 286–291, https://doi.org/10.1016/J.PHPRO. 2011.11.045.

[30] B.H. Mo, H. Zhu, X.M. Cui, Y. He, S.Y. Gong, Effect of curing temperature on geopolymerization of metakaolin-based geopolymers, Appl. Clay Sci. 99 (2014) 144–148, https://doi.org/10.1016/J.CLAY.2014.06.024.

[31] M. Kaya, M. Uysal, K. Yilmaz, O. Karahan, C.D. Atis, Mechanical properties of class C and F fly ash geopolymer mortars, Gradjevinar 72 (2020) 297–309, https://doi.org/10.14256/JCE.2421.2018.

[32] O.K. Wattimena, D. Hardjito Antoni, A review on the effect of fly ash characteristics and their variations on the synthesis of fly ash based geopolymer, AIP Conf. Proc. 1887 (2017), 020041, https://doi.org/10.1063/1.5003524.

[33] L. Biondi, M. Perry, C. Vlachakis, Z. Wu, A. Hamilton, J. McAlorum, Ambient cured fly ash geopolymer coatings for concrete, Materials 12 (2019) 923, https://doi.org/10.3390/MA12060923, 12 (2019) 923.

[34] M.H. Al-Majidi, A. Lampropoulos, A. Cundy, S. Meikle, Development of geopolymer mortar under ambient temperature for in situ applications, Construct. Build. Mater. 120 (2016) 198–211, https://doi.org/10.1016/J.CONBUILDMAT.2016.05.085.

[35] P. Nath, P.K. Sarker, V.B. Rangan, Early age properties of low-calcium fly ash geopolymer concrete Suitable for ambient curing, Procedia Eng. 125 (2015) 601–607, https://doi.org/10.1016/J.PROENG.2015.11.077.

[36] H. Shinde, N. Kadam, Effect of addition of ordinary portland cement on geopolymer concrete with ambient curing, Int. J. Mod. Trends Eng. Res. (2016) 28–30.

[37] B.B. Jindal, D. Singhal, S. Sharma, Parveen, Enhancing mechanical and durability properties of geopolymer concrete with mineral admixture, Comput. Concr. 21 (2018) 345–353, https://doi.org/10.12989/CAC.2018.21.3.345.

[38] D. Adak, M. Sarkar, S. Mandal, Effect of nano-silica on strength and durability of fly ash based geopolymer mortar, Construct. Build. Mater. 70 (2014) 453–459, https://doi.org/10.1016/J.CONBUILDMAT.2014.07.093.

[39] P. Chindaprasirt, S. Rukzon, Strength, porosity and corrosion resistance of ternary blend Portland cement, rice husk ash and fly ash mortar, Construct. Build. Mater. 22 (2008) 1601–1606, https://doi.org/10.1016/J.CONBUILDMAT.2007.06.010.

[40] A. Wardhono, Y. Risdianto, M.F. Sofianto, M.T. Nur, A.H. Pradipta, The strength properties of high calcium fly ash geopolymer specimens incorporating mud-volcanic and limestone variations, IOP Conf. Ser. Mater. Sci. Eng. 669 (2019), 012016, https://doi.org/10.1088/1757-899X/669/1/012016.

[41] Z.H. Zhang, X. Yao, H.J. Zhu, S.D. Hua, Y. Chen, Preparation and mechanical properties of polypropylene fiber reinforced calcined kaolin-fly ash based geopolymer, J. Cent. South Univ. Technol. 161 (2009) 49–52, https://doi.org/10.1007/S11771-009-0008-4, 16 (2009.

[42] Selamawit, Teff Straw Ash as Partial Cement Replacement Material, Addis Ababa University, Ethiopia, 2020. Unpublished master's thesis.

[43] A.B. Wassie, V.C. Srivastava, Teff straw characterization and utilization for chromium removal from wastewater: kinetics, isotherm and thermodynamic modelling, J. Environ. Chem. Eng. 4 (2016) 1117–1125, https://doi.org/10.1016/J.JECE.2016.01.019.

[44] A. Chufo, H. Yuan, D. Zou, Y. Pang, X. Li, Biomethane production and physicochemical characterization of anaerobically digested teff (Eragrostis tef) straw pretreated by sodium hydroxide, Bioresour. Technol. 181 (2015) 214–219, https://doi.org/10.1016/J.BIORTECH.2015.01.054.

[45] A.L. Ayele, B.Z. Tizazu, A.B. Wassie, Chemical modification of teff straw biomass for adsorptive removal of Cr (VI) from aqueous solution: characterization, optimization, kinetics, and thermodynamic aspects, Adsorpt. Sci. Technol. 2022 (2022), https://doi.org/10.1155/2022/5820207.

[46] A.B. Wassie, V.C. Srivastava, Chemical treatment of teff straw by sodium hydroxide, phosphoric acid and zinc chloride: adsorptive removal of chromium, Int. J. Environ. Sci. Technol. 13 (2016) 2415–2426, https://doi.org/10.1007/S13762-016-1080-6.

[47] A.B. Bageru, V.C. Srivastava, Preparation and characterisation of biosilica from teff (eragrostis tef) straw by thermal method, Mater. Lett. 206 (2017) 13–17, https://doi.org/10.1016/J.MATLET.2017.06.100.

[48] A.K. Tadesse, Experimental study on mechanical properties of teff straw as a fiber in reinforced concrete, Glob. Sci. J. 7 (2019) 123–139.

[49] ASTM C188-03, Standard Test Method for Density of Hydraulic Cement, ASTM International, West Conshohocken, PA, USA, 2003.

[50] Astm C 311-08, Standard Test Methods for Sampling and Testing Fly Ash or Natural Pozzolans for Use in Portland-Cement Concrete, ASTM International, West Conshohocken, PA, USA, 2008.

[51] ASTM D422-03, Standard Test Method for Particle-Size Analysis of Soils, ASTM International, West Conshohocken, PA, USA, 2003.

[52] ASTM C618-08, Standard Specification for Coal Fly Ash and Raw or Calcined Natural Pozzolan for use in Concrete, ASTM International, West Conshohocken, PA, USA, 2008.

[53] ASTM C128-07, Standard Test Method for Density, Relative Density (Specific Gravity), and Absorption of Coarse Aggregate, ASTM International, West Conshohocken, PA, USA, 2007.

[54] ASTM C136-08, Standard Test Method for Sieve Analysis of Fine and Coarse Aggregates, ASTM International, West Conshohocken, PA, USA, 2011.

[55] ASTM C33/C33M-08, Standard Specification for Concrete Aggregates, ASTM International, West Conshohocken, PA, USA, 2009.

[56] A.Z.W. Wazien, M.M.A.B. Abdullah, R. Abd Razak, M.A.Z.M.R. Rozainy, M.F. M. Tahir, Strength and density of geopolymer mortar cured at ambient temperature for use as repair material, IOP Conf. Ser. Mater. Sci. Eng. 133 (2016), 012042, https://doi.org/10.1088/1757-899X/133/1/012042.

[57] O. Abiodun, C. Kabubo, R. Mutuku, O. Ejohwomu, The effect of Pristine graphene on the mechanical properties of geopolymer mortar, Sustain. Times 15 (2023) 1706, https://doi.org/10.3390/SU15021706, 15 (2023) 1706.

[58] S. Hanjitsuwan, S. Hunpratub, P. Thongbai, S. Maensiri, V. Sata, P. Chindaprasirt, Effects of NaOH concentrations on physical and electrical properties of high calcium fly ash geopolymer paste, Cem. Concr. Compos. 45 (2014) 9–14, https://doi.org/10.1016/J.CEMCONCOMP.2013.09.012.

[59] ASTM C1437-07, Standard Test Method for Flow of Hydraulic Cement Mortar, ASTM International, West Conshohocken, PA, USA, 2007.

[60] ASTM C109/109M-08, Standard Test Method for Compressive Strength of Hydraulic Cement Mortars, ASTM International, West Conshohocken, PA, USA, 2009.

[61] ASTM C348-08, Standard Test Method for Flexural Strength of Hydraulic-Cement Mortars, ASTM International, West Conshohocken, PA, USA, 2009.

[62] ASTM C307-03, Standard Test Method for Tensile Strength of Chemical- Resistant Mortar, Grouts, and Monolithic Surfacings, ASTM International, West Conshohocken, PA, USA, 2008.

[63] S. Kumar Das, A. Adediran, C. Rodrigue Kaze, S. Mohammed Mustakim, N. Leklou, Production, characteristics, and utilization of rice husk ash in alkali activated materials: an overview of fresh and hardened state properties, Construct. Build. Mater. 345 (2022), 128341, https://doi.org/10.1016/J.CONBUILDMAT.2022.128341.

[64] M.Z. Zaidahtulakmal, K. Kartini, M.S. Hamidah, S. Alam, Rice husk ash (RHA) based geopolymer mortar incorporating sewage sludge ash (SSA), J. Phys. Conf. Ser. 1349 (2019), 12022, https://doi.org/10.1088/1742-6596/1349/1/012022.

[65] S. Detphan, P. Chindaprasirt, Preparation of fly ash and rice husk ash geopolymer, Int. J. Miner. Metall. Mater. 16 (2009) 720–726, https://doi.org/10.1016/S1674-4799(10)60019-2.

[66] Q. Li, S. Chen, Y. Zhang, Y. Hu, Q. Wang, Q. Zhou, Y. Yan, Y. Liu, D. Yan, Effect of curing temperature on high-strength metakaolin-based geopolymer composite (HMGC) with quartz powder and Steel fibers, Materials 15 (2022), https://doi.org/10.3390/MA15113958.

[67] L. Assi, S.A. Ghahari, E.E. Deaver, D. Leaphart, P. Ziehl, Improvement of the early and final compressive strength of fly ash-based geopolymer concrete at ambient conditions, Construct. Build. Mater. 123 (2016) 806–813, https://doi.org/10.1016/J.CONBUILDMAT. 2016.07.069.

[68] P. Baskar, S. Annadurai, K. Sekar, M. Prabakaran, A review on fresh, hardened, and microstructural properties of fibre-reinforced geopolymer concrete, Polymers 15 (2023) 1484, https://doi.org/10.3390/POLYM15061484, 15 (2023) 1484.

[69] P. Chindaprasirt, T. Chareerat, S. Hatanaka, T. Cao, High-strength geopolymer using fine high-calcium fly ash, J. Mater. Civ. Eng. 23 (2011) 264–270, https://doi.org/10.1061/(ASCE)MT.1943-5533.0000161.

[70] O.A. Abdulkareem, M. Ramli, J.C. Matthews, Production of geopolymer mortar system containing high calcium biomass wood ash as a partial substitution to fly ash: an early age evaluation, Compos. B Eng. 174 (2019), 106941, https://doi.org/10.1016/J. COMPOSITESB.2019.106941.

[71] A. Hajimohammadi, J.L. Provis, J.S.J. Van Deventer, The effect of silica availability on the mechanism of geopolymerisation, Cem. Concr. Res. 41 (2011) 210–216, https://doi.org/10.1016/J.CEMCONRES.2011.02.001.

[72] A. Fernández-Jiménez, A. Palomo, Characterisation of fly ashes. Potential reactivity as alkaline cements, Fuel 82 (2003) 2259–2265, https://doi.org/10.1016/S0016-2361(03) 00194-7.

[73] E. Álvarez-Ayuso, X. Querol, F. Plana, A. Alastuey, N. Moreno, M. Izquierdo, O. Font, T. Moreno, S. Diez, E. Vázquez, M. Barra, Environmental, physical and structural characterisation of geopolymer matrixes synthesised from coal (co-) combustion fly ashes, J. Hazard Mater. 154 (2008) 175–183, https://doi.org/10.1016/J.JHAZMAT.2007.10.008.

[74] M. Kaya, O. Karahan, C.D. Atiş, Influence of silica fume additive and activator ratio on mechanical properties in slaked lime-based alkali-activated mortars, Iran, J. Sci. Technol. Trans. Civ. Eng. 47 (2022) 873–889, https://doi.org/10.1007/S40996-022-009 60-4/METRICS.

[75] N. Ranjbar, M. Mehrali, A. Behnia, U.J. Alengaram, M.Z. Jumaat, Compressive strength and microstructural analysis of fly ash/palm oil fuel ash based geopolymer mortar, Mater. Des. 59 (2014) 532–539, https://doi.org/10.1016/J.MATDES.2014.03.037.

[76] 16 rue Galilée, 02100 Saint-Quentin, France geopolymer institute, geopolymers: ceramic-like inorganic Polymers, J. Ceram. Sci. Technol. 8 (2017) 335–350, https://doi.org/10.4416/JCST2017-00038.

[77] S.A. Bernal, J.L. Provis, V. Rose, R. Mejía De Gutierrez, Evolution of binder structure in sodium silicate-activated slag-metakaolin blends, Cem. Concr. Compos. 33 (2011) 46–54, https://doi.org/10.1016/J.CEMCONCOMP.2010.09.004.

[78] X. Yang, Y. Zhang, C. Lin, Compressive and flexural properties of ultra-fine coal gangue-based geopolymer gels and microscopic mechanism analysis, Gels 8 (2022) 145, https://doi.org/10.3390/GELS8030145, 8 (2022) 145.

[79] F. Puertas, M. Palacios, H. Manzano, J.S. Dolado, A. Rico, J. Rodríguez, A model for the C-A-S-H gel formed in alkali-activated slag cements, J. Eur. Ceram. Soc. 31 (2011) 2043–2056, https://doi.org/10.1016/J.JEURCERAMSOC.2011.04.036.

[80] I. García Lodeiro, A. Fernández-Jimenez, A. Palomo, D.E. Macphee, Effect on fresh C-S-H gels of the simultaneous addition of alkali and aluminium, Cem. Concr. Res. 40 (2010) 27–32, https://doi.org/10.1016/J.CEMCONRES.2009.08.004.

[81] S.A. Bernal, J.L. Provis, B. Walkley, R. San Nicolas, J.D. Gehman, D.G. Brice, A. R. Kilcullen, P. Duxson, J.S.J. Van Deventer, Gel nanostructure in alkali-activated binders based on slag and fly ash, and effects of accelerated carbonation, Cem. Concr. Res. 53 (2013) 127–144, https://doi.org/10.1016/J.CEMCONRES.2013.06.007.

[82] Q. Lv, J. Yu, F. Ji, L. Gu, Y. Chen, X. Shan, Mechanical property and microstructure of fly ash-based geopolymer activated by sodium silicate, KSCE J. Civ. Eng. 25 (2021) 1765–1777, https://doi.org/10.1007/S12205-021-0025-X/METRICS.

[83] C. Ng, U.J. Alengaram, L.S. Wong, K.H. Mo, M.Z. Jumaat, S. Ramesh, A review on microstructural study and compressive strength of geopolymer mortar, paste and concrete, Construct. Build. Mater. 186 (2018) 550–576, https://doi.org/10.1016/J.CONBUILDMAT.2018.07.075.

[84] J.G. Jang, N.K. Lee, H.K. Lee, Fresh and hardened properties of alkali-activated fly ash/slag pastes with superplasticizers, Construct. Build. Mater. 50 (2014) 169–176, https://doi.org/10.1016/J.CONBUILDMAT.2013.09.048.